

---

This is an electronic reprint of the original article.  
This reprint may differ from the original in pagination and typographic detail.

Graubner, Tim; Rudel, Stefan S.; Ivlev, Sergei I.; Karttunen, Antti J.; Kraus, Florian  
**Uranium Cyanides from Reactions in Liquid Ammonia Solution**

*Published in:*  
European Journal of Inorganic Chemistry

*DOI:*  
[10.1002/ejic.202400041](https://doi.org/10.1002/ejic.202400041)

Published: 03/06/2024

*Document Version*  
Publisher's PDF, also known as Version of record

*Published under the following license:*  
CC BY

*Please cite the original version:*  
Graubner, T., Rudel, S. S., Ivlev, S. I., Karttunen, A. J., & Kraus, F. (2024). Uranium Cyanides from Reactions in Liquid Ammonia Solution. *European Journal of Inorganic Chemistry*, 27(16), Article e202400041.  
<https://doi.org/10.1002/ejic.202400041>

---

This material is protected by copyright and other intellectual property rights, and duplication or sale of all or part of any of the repository collections is not permitted, except that material may be duplicated by you for your research use or educational purposes in electronic or print form. You must obtain permission for any other use. Electronic or print copies may not be offered, whether for sale or otherwise to anyone who is not an authorised user.

## Hot Paper

## Uranium Cyanides from Reactions in Liquid Ammonia Solution

Tim Graubner,<sup>[a]</sup> Stefan S. Rudel,<sup>[a]</sup> Sergei I. Ivlev,<sup>[a]</sup> Antti J. Karttunen,<sup>[b]</sup> and Florian Kraus<sup>\*[a]</sup>

Reactions of uranium tri- and tetrahalides,  $\text{UBr}_3$ ,  $\text{UI}_3$ ,  $\text{UCl}_4$ , and  $\text{U}_4$ , with different cyanides  $\text{MCN}$  ( $M = \text{K}, \text{Ag}$ ) in liquid anhydrous ammonia led to three novel uranium(IV) cyanide compounds. The reaction of  $\text{UCl}_4$  in the presence of KCN resulted in the compound  $[\text{U}(\text{CN})(\text{NH}_3)_8]\text{Cl}_3 \cdot 3\text{NH}_3$ , while  $\text{UBr}_3$  and  $\text{UI}_3$  were oxidized in the presence of AgCN to form the compounds  $[\infty^1[(\mu\text{-CN})\{(\text{H}_3\text{N})_5\text{U}(\mu\text{-NH}_2)_3\text{U}(\text{NH}_3)_5\}]\text{Br}_4 \cdot 2\text{NH}_3$ , and  $[\infty^1[(\mu\text{-CN})\{(\text{H}_3\text{N})_5\text{U}(\mu\text{-NH}_2)_3\text{U}(\text{NH}_3)_5\}]\text{I}_4 \cdot 2\text{NH}_3$ . The reaction of  $\text{U}_4$  with KCN in  $\text{aNH}_3$  also yielded the compound  $[\infty^1[(\mu\text{-CN})\{(\text{H}_3\text{N})_5\text{U}(\mu\text{-NH}_2)_3\text{U}(\text{NH}_3)_5\}]\text{I}_4 \cdot 2\text{NH}_3$ . The compounds  $[\infty^1[(\mu\text{-CN})\{(\text{H}_3\text{N})_5\text{U}(\mu\text{-NH}_2)_3\text{U}(\text{NH}_3)_5\}]\text{X}_4 \cdot 2\text{NH}_3$  ( $\text{X} = \text{Br}, \text{I}$ ) crystallize in different space groups,  $Pmn2_1$  (no. 31) and  $Immm2$  (no. 44), respectively. In both cases, the  $[\infty^1[(\mu\text{-CN})\{(\text{H}_3\text{N})_5\text{U}(\mu\text{-NH}_2)_3\text{U}(\text{NH}_3)_5\}]\text{X}_4 \cdot 2\text{NH}_3$  cation forms infinite strands. We conducted quantum-chemical calculations and Intrinsic Bond Orbital analyses on the observed  $[\text{U}(\text{CN})(\text{NH}_3)_8]^{3+}$  cation and the  $[(\mu\text{-CN})_2\{(\text{H}_3\text{N})_5\text{U}(\mu\text{-NH}_2)_3\text{U}(\text{NH}_3)_5\}]^{3+}$  model cation to gain insight into the bonding situation.

Here we report on the syntheses and crystal structures of the compounds  $[\text{U}(\text{CN})(\text{NH}_3)_8]\text{Cl}_3 \cdot 3\text{NH}_3$ ,  $[\infty^1[(\mu\text{-CN})\{(\text{H}_3\text{N})_5\text{U}(\mu\text{-NH}_2)_3\text{U}(\text{NH}_3)_5\}]\text{Br}_4 \cdot 2\text{NH}_3$ , and  $[\infty^1[(\mu\text{-CN})\{(\text{H}_3\text{N})_5\text{U}(\mu\text{-NH}_2)_3\text{U}(\text{NH}_3)_5\}]\text{I}_4 \cdot 2\text{NH}_3$ .

## Introduction

Uranium cyanides are a little-known class of substances. Neither a pseudobinary U cyanide like  $\text{U}(\text{CN})_4$  nor a homoleptic cyanido complex such as for example  $[\text{U}(\text{CN})_6]^{4-}$  are known to date. However, corresponding complex anions have been reported for the somewhat related elements Mo and W.<sup>[1]</sup> As oxidation state +IV is quite stable for U and the halides  $\text{UX}_4$  ( $\text{X} = \text{F} - \text{I}$ ) are well characterized, we have set ourselves the goal of synthesizing U(IV) cyanides. In liquid anhydrous ammonia ( $\text{aNH}_3$ ) as a solvent, a previous report on the reaction of  $\text{UCl}_4$  with NaCN claimed the synthesis of  $[\text{UCl}_3(\text{CN})] \cdot 4\text{NH}_3$  which had been characterized by infrared spectroscopy.<sup>[2]</sup> Another U–CN containing compound obtained from reactions in liquid  $\text{aNH}_3$  is  $[\text{U}_2(\text{CN})_3(\text{NH}_3)_{14}][\text{KBr}_6] \cdot \text{NH}_3$ , where the U atoms are bridged by  $\text{CN}^-$  ligands to form a layer structure.<sup>[3]</sup> In an attempt to make a U cyanide, the compound  $[\text{UCl}_4(\text{HCN})_4]$  was obtained from the reaction of  $\text{UCl}_4$  in anhydrous HCN.<sup>[4]</sup> Thermal decomposition led back to the starting materials. In a review article,<sup>[5]</sup> the compounds of  $[\text{U}(\text{CN})(\text{NH}_3)_8]\text{Cl}_3 \cdot 3\text{NH}_3$ ,  $[\infty^1[(\mu\text{-CN})\{(\text{H}_3\text{N})_5\text{U}(\mu\text{-NH}_2)_3\text{U}(\text{NH}_3)_5\}]\text{I}_4 \cdot 2\text{NH}_3$ , and  $[\text{U}(\text{CN})_3(\text{NH}_3)_6]$  were only briefly mentioned without providing structural data.

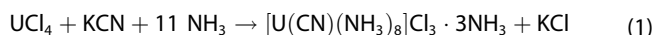
From reactions of uranium tri- and tetrahalides,  $\text{UBr}_3$ ,  $\text{UI}_3$ ,  $\text{UCl}_4$ , and  $\text{U}_4$ , with the cyanides KCN or AgCN in liquid  $\text{aNH}_3$  solution, we obtained compounds containing a monocyanidouranium(IV) complex cation or two structurally related  $(\mu\text{-NH}_2)_3^-$  and  $\mu\text{-CN}^-$ -bridged uranium(IV) compounds. Scheme 1 shows the carried-out reactions, their conditions as well as the products. See the Experimental Part for more details.

## Results and Discussion

From the reaction of  $\text{UCl}_4$  with one equivalent of KCN in liquid  $\text{aNH}_3$  at room temperature, we observed the formation of green plate-shaped crystals after six months of crystallization time. A single-crystal X-ray structure analysis showed the composition  $[\text{U}(\text{CN})(\text{NH}_3)_8]\text{Cl}_3 \cdot 3\text{NH}_3$ , octaamminemonocyanidouranium(IV) chloride–ammonia(1/3). Its formation can be described by equation 1.

Synthesis and structural characterization of  $[\text{U}(\text{CN})(\text{NH}_3)_8]\text{Cl}_3 \cdot 3\text{NH}_3$ 

The formation of KCl was evidenced by its powder X-ray diffraction pattern recorded on the dried residue obtained after removal of the liquid  $\text{aNH}_3$  from the reaction mixture. The diffraction pattern is shown in Figure S5 of the Supporting Information.



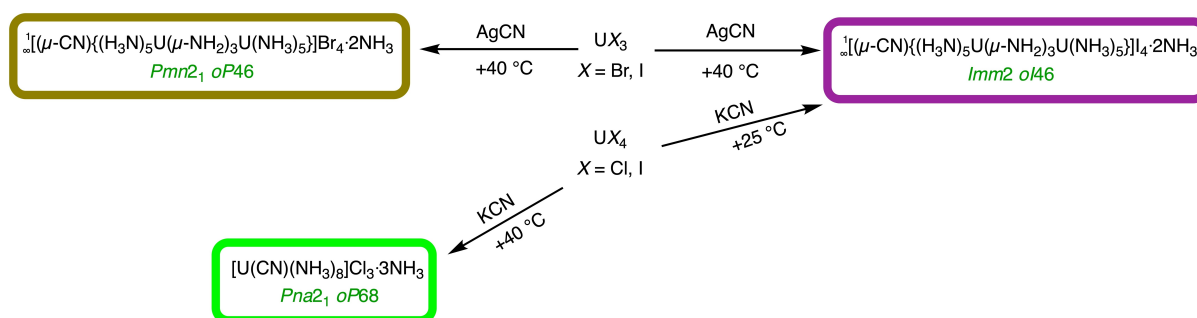
In the absence of cyanide ions, the ammonolysis product of  $\text{UCl}_4$  was shown to be the composition-wise related

[a] T. Graubner, Dr. S. S. Rudel, Dr. S. I. Ivlev, Prof. Dr. F. Kraus  
Fluorchemie, Fachbereich Chemie, Philipps-Universität Marburg,  
Hans-Meerwein-Str. 4, 35032 Marburg (Germany)  
E-mail: F.kraus@uni-marburg.de  
Homepage: [http://www.uni-marburg.de/de/fb15/arbeitsgruppen/anorganische\\_chemie/ag-kraus](http://www.uni-marburg.de/de/fb15/arbeitsgruppen/anorganische_chemie/ag-kraus)

[b] Prof. Dr. A. J. Karttunen  
Department of Chemistry and Materials Science, Aalto University, Kemistintie 1, FI-02150 Espoo (Finland)

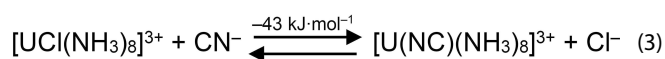
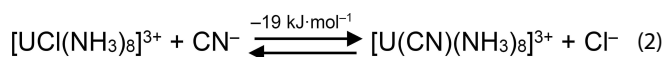
Supporting information for this article is available on the WWW under <https://doi.org/10.1002/ejic.202400041>

© 2024 The Authors. European Journal of Inorganic Chemistry published by Wiley-VCH GmbH. This is an open access article under the terms of the Creative Commons Attribution License, which permits use, distribution and reproduction in any medium, provided the original work is properly cited.



**Scheme 1.** An overview of the compounds reported here in boxes and the reaction conditions for their formation. Chlorides in the green, bromides in the brown, and iodides in the purple boxes. Space groups and Pearson symbols, without H atoms, are given for easier comparison of the crystal structures.

$[\text{U}(\text{NH}_3)_8]\text{Cl}_3 \cdot 3\text{NH}_3$ .<sup>[5]</sup> Nonetheless, species that are formed in solution as intermediates are unknown as of yet. It is therefore possible that in the presence of cyanide ions the  $[\text{UCl}(\text{NH}_3)_8]^{3+}$  and the  $[\text{U}(\text{CN})(\text{NH}_3)_8]^{3+}$  cations are in chemical equilibrium with each other. A putative ligand exchange reaction can be formulated as follows in equations 2 and 3. Both linkage-isomers of the  $\text{CN}^-$  ligands were considered.



The values of  $-19 \text{ kJ}\cdot\text{mol}^{-1}$  and  $-43 \text{ kJ}\cdot\text{mol}^{-1}$  on the reaction arrows are the calculated reaction energies at the DFT-PBE0/TZVP level of theory for the complex cations at 0 K (in COSMO continuum solvent field). See the computational details for more details. The exchange reaction slightly favors the formation of the  $[\text{U}(\text{CN})(\text{NH}_3)_8]^{3+}$  cation energetically with  $19 \text{ kJ}\cdot\text{mol}^{-1}$ . In comparison, the  $[\text{U}(\text{NC})(\text{NH}_3)_8]^{3+}$  cation is more favored, with  $43 \text{ kJ}\cdot\text{mol}^{-1}$ . When considering Gibbs Free Energies at 298 K, the left side of equation 2 is favored by  $34 \text{ kJ}\cdot\text{mol}^{-1}$ . For equation 3, the left side is favored with  $11 \text{ kJ}\cdot\text{mol}^{-1}$ . In conclusion, this suggests a strong thermal dependency of the exchange reaction, valid for both linkage-isomers. The energy difference between both linkage-isomers  $[\text{U}(\text{CN})(\text{NH}_3)_8]^{3+}$  and  $[\text{U}(\text{NC})(\text{NH}_3)_8]^{3+}$  is  $23 \text{ kJ}\cdot\text{mol}^{-1}$ , favoring the latter.

$[\text{U}(\text{CN})(\text{NH}_3)_8]\text{Cl}_3 \cdot 3\text{NH}_3$  crystallizes in the orthorhombic crystal system, space group  $Pna2_1$  (no. 33), with the lattice parameters  $a = 8.2426(2)$ ,  $b = 14.2004(4)$ ,  $c = 16.6927(6) \text{ \AA}$ ,  $V = 1953.85(10) \text{ \AA}^3$ , and  $Z = 4$ , at  $T = 100 \text{ K}$ . The diffraction pattern of the crystal appeared to be non-merohedrally twinned, but only the main domain was used during integration of the dataset and for the solution and refinement of the crystal structure model, see the Experimental Section and Table 1 for details. The Supporting Information also contains an explanation for the selection of the space group  $Pna2_1$  over  $Pnma$  and less likely alternatives.

The crystal structure contains one symmetry-independent U atom ( $4c$ ,  $.m$ ) which is surrounded by eight  $\text{NH}_3$  ligands and

one disordered  $\text{NC}^-/\text{CN}^-$  ligand to form a tricapped trigonal prism-like coordination sphere. The C and N atoms in the  $\text{CN}^-$  unit are statistically disordered, with a 50:50 mixed site occupancy and in the following the  $\text{NC}/\text{CN}^-$  unit will be written as  $\text{CN}^-$ . See the Supporting Information for more crystallographic details.

The molecular structure of the  $[\text{U}(\text{CN})(\text{NH}_3)_8]^{3+}$  cation in its salt is shown in Figure 1.

The U– $\text{NH}_3$  distances are with  $2.531(16)$  to  $2.595(5) \text{ \AA}$  in the expected range and agree to those within the  $[\text{U}(\text{NH}_3)_{10}]^{4+}$  cation with  $2.5390(15)$  to  $2.621(2) \text{ \AA}$  where however a bicapped-square antiprismatic coordination sphere is present.<sup>[6]</sup> The two longer U–N bonds are  $2.654(2)$  and  $2.881(4) \text{ \AA}$ .<sup>[6]</sup>

The U–C/N bond has a length of  $2.585(6) \text{ \AA}$ . Due to the lack of comparable structures of mononuclear uranium ammine complexes containing terminally bound  $\text{CN}^-$  ligands, we calculated both linkage-isomers,  $\kappa\text{C}$  and  $\kappa\text{N}$ , of the  $[\text{U}(\text{CN})(\text{NH}_3)_8]^{3+}$  cation at the DFT-PBE0/TZVP level of theory. The calculated U–CN and U–NC bond lengths are  $2.511$  and  $2.395 \text{ \AA}$ , respectively. These distances are shortened for both linkage-isomers, in comparison to the experimentally observed

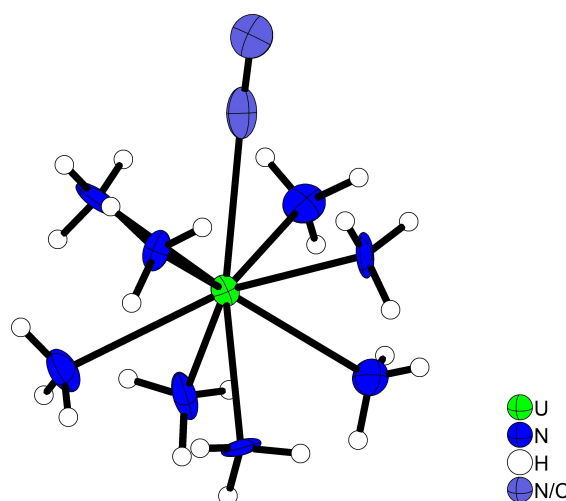


**Figure 1.** Molecular structure of the  $[\text{U}(\text{CN})(\text{NH}_3)_8]^{3+}$  cation in the compound  $[\text{U}(\text{CN})(\text{NH}_3)_8]\text{Cl}_3 \cdot 3\text{NH}_3$ . Atoms are shown with anisotropic displacement ellipsoids at the 70% probability level at 100 K and H atoms are shown isotropic with arbitrary radii.

**Table 1.** Selected crystallographic data and details of the structure determinations of  $[\text{U}(\text{CN})(\text{NH}_3)_8]\text{Cl}_3 \cdot 3\text{NH}_3$ ,  $[\text{U}(\text{CN})(\text{NH}_3)_8]\text{Cl}_3 \cdot 3\text{NH}_3$ ,  $[\text{U}(\text{CN})(\text{NH}_3)_8]\text{Cl}_3 \cdot 3\text{NH}_3$ , and  $[\text{U}(\text{CN})(\text{NH}_3)_8]\text{Cl}_3 \cdot 3\text{NH}_3$ .

Compound	$[\text{U}(\text{CN})(\text{NH}_3)_8]\text{Cl}_3 \cdot 3\text{NH}_3$	$[\text{U}(\text{CN})(\text{NH}_3)_8]\text{Cl}_3 \cdot 3\text{NH}_3$	$[\text{U}(\text{CN})(\text{NH}_3)_8]\text{Cl}_3 \cdot 3\text{NH}_3$
Formula	$\text{UCl}_3\text{N}_{12}\text{CH}_{33}$	$\text{U}_2\text{Br}_4\text{N}_{16}\text{CH}_{39}$	$\text{U}_2\text{I}_4\text{N}_{16}\text{CH}_{39}$
Molar mass/g·mol <sup>-1</sup>	557.77	1057.14	1262.16
Space group (No.)	<i>Pna</i> 2 <sub>1</sub> (33)	<i>Pmn</i> 2 <sub>1</sub> (31)	<i>Imm</i> 2 (44)
<i>a</i> /Å	8.2426(2)	10.0381(3)	13.6703(9)
<i>b</i> /Å	14.2004(4)	12.8196(4)	10.1319(6)
<i>c</i> /Å	16.6927(6)	10.8057(4)	10.8507(7)
<i>V</i> /Å <sup>3</sup>	1953.85(10)	1390.53(8)	1502.89(16)
<i>Z</i>	4	2	2
Pearson symbol	<i>oP</i> 68 (w/o H atoms)	<i>oP</i> 46 (w/o H atoms)	<i>oI</i> 46 (w/o H atoms)
$\rho_{\text{calc}}/\text{g}\cdot\text{cm}^{-3}$	1.896	2.551	2.789
$\mu/\text{mm}^{-1}$	8.722	17.396	14.888
Color	green	green	green
Crystal morphology	plate	block	block
Crystal size/mm <sup>3</sup>	0.20×0.20×0.05	0.168×0.125×0.068	0.143×0.075×0.052
<i>T</i> /K	100	100	100
$\lambda/\text{Å}$	0.71073 (MoK $\alpha$ )	0.71073 (MoK $\alpha$ )	0.71073 (MoK $\alpha$ )
No. of reflections	17775	83849	40306
$\theta$ range/°	3.474–30.502	2.465–36.419	2.396–36.305
Range of Miller indices	$-10 \leq h \leq 11$ $-20 \leq k \leq 14$ $-19 \leq l \leq 23$	$-16 \leq h \leq 16$ $-21 \leq k \leq 21$ $-18 \leq l \leq 18$	$-22 \leq h \leq 22$ $-16 \leq k \leq 16$ $-18 \leq l \leq 18$
Absorption correction	multi-scan and numerical	multi-scan and numerical	multi-scan and numerical
$T_{\text{max}}, T_{\text{min}}$	0.5235, 0.1368	0.4530, 0.2555	0.2880, 0.1750
$R_{\text{int}}, R_{\sigma}$	0.0294, 0.0203	0.0306, 0.0198	0.0322, 0.0231
Completeness of the data set	0.894	0.999	0.998
No. of unique reflections	6384	7056	3758
No. of parameters, restraints	159, 1	117, 0	81, 7
<i>S</i> (all data)	1.083	1.056	1.194
<i>R</i> ( <i>F</i> ) ( $I \geq 2\sigma(I)$ , all data)	0.0339, 0.0389	0.0154, 0.0195	0.0145, 0.0147
<i>wR</i> ( <i>F</i> <sup>2</sup> ) ( $I \geq 2\sigma(I)$ , all data)	0.0762, 0.0782	0.0382, 0.0400	0.0351, 0.0351
Extinction coefficient	–	–	0.00033(7)
Flack parameter	BASF: 0.52(2)	0.030(6)	0.062(5)
$\Delta\rho_{\text{max}}, \Delta\rho_{\text{min}}/\text{e}\cdot\text{Å}^{-3}$	3.445, –2.254	3.215, –1.033	3.379, –1.002

value. Selected experimentally determined bond lengths for the  $[\text{U}(\text{CN})(\text{NH}_3)_8]^{3+}$  cation are compared to the calculated ones at the DFT-PBE0/TZVP level of theory in Table S6 of the Supporting Information.

The C–N bond length has a value of 1.109(9) Å, which agrees with previously reported distances of 1.11(3) Å in  $[\text{U}_2(\text{CN})_3(\text{NH}_3)_{14}][\text{KBr}_6]$  and 1.16(1) in KCN.<sup>[3,7]</sup> In comparison to the experimentally determined value, the results from DFT agree with 1.160 and 1.168 Å for the U–CN and U–NC, respectively.

A description of the coordination sphere of the anions, hydrogen bonding, and a packing analysis of the crystal structure is available in the Supporting Information.

A closer look at the U–C/N bonding situation in the  $[\text{U}(\text{CN})(\text{NH}_3)_8]^{3+}$  cation was taken with the help of calculations at the DFT-PBE0/TZVP level of theory using the Intrinsic Bond Orbital (IBO) analysis.<sup>[8]</sup> One  $\sigma$ -type IBO describing the U–C/N bond, while no IBO related to a  $\pi$ -type backbond was not observed. The IBOs of both linkage-isomers,  $\kappa\text{N}$  and  $\kappa\text{C}$ , are compared with each other in Figure 2, with the respective contributions of the U and C or N atom. A detailed discussion on the orbital contributions is handed in the IBO section of the Supporting Information.

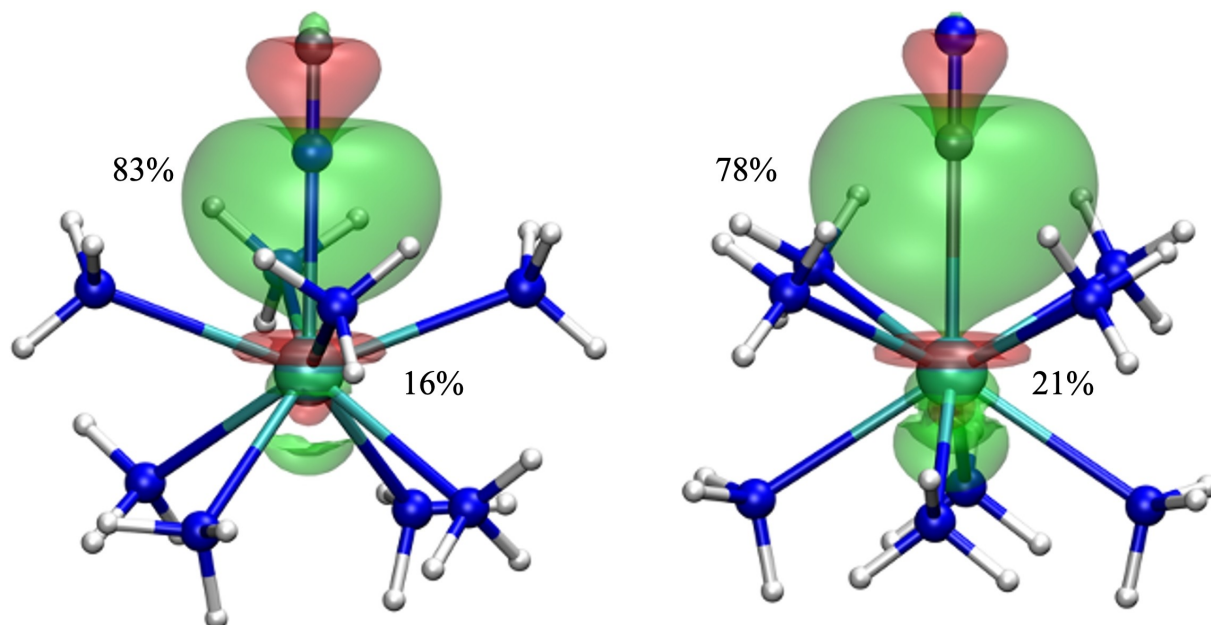
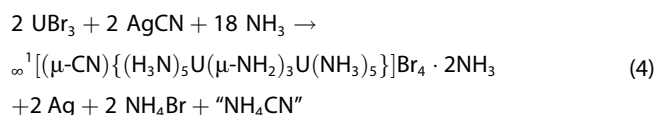


**Figure 2.** Two IBOs for the  $[\text{U}(\text{CN})(\text{NH}_3)_9]^{3+}$  cation (isosurfaces drawn in green and red). Left: IBO showing one the  $\sigma$ -type bond between U–NC. Right: IBO showing one the  $\sigma$ -type bond between U–CN. The listed percentages show the contribution of each atom in the IBO. In a purely covalent 2c-bond, each atom would contribute 50%. Atomic contributions smaller than 2% to any IBO are not listed. The isovalue for IBO isosurface plots is 0.03 a.u. U atoms in cyan, N atoms in blue, O atoms in red, and H atoms in white color.

### Synthesis and structural characterization of $\infty^1[(\mu\text{-CN})\{(\text{H}_3\text{N})_5\text{U}(\mu\text{-NH}_2)_3\text{U}(\text{NH}_3)_5\}]\text{Br}_4 \cdot 2\text{NH}_3$

From the reaction of  $\text{UBr}_3$  with  $\text{AgCN}$  in liquid  $\text{aNH}_3$  at  $+40^\circ\text{C}$  in bomb tubes, we obtained green crystals after 10 months of crystallization time for which single-crystal structure analysis led to the composition  $\infty^1[(\mu\text{-CN})\{(\text{H}_3\text{N})_5\text{U}(\mu\text{-NH}_2)_3\text{U}(\text{NH}_3)_5\}]\text{Br}_4 \cdot 2\text{NH}_3$ . The formation of the compound can be described by equation 4.



The side products,  $\text{Ag}$  and  $\text{NH}_4\text{Br}$ , have been identified by powder X-ray diffraction of the dried left-overs of  $\infty^1[(\mu\text{-CN})\{(\text{H}_3\text{N})_5\text{U}(\mu\text{-NH}_2)_3\text{U}(\text{NH}_3)_5\}]\text{Br}_4 \cdot 2\text{NH}_3$  after evaporation of the liquid  $\text{aNH}_3$ . The diffraction pattern is shown in Figure S6 of the Supporting Information. For the balance of the reaction equation, another product is needed to account for the missing  $\text{CN}^-$  unit. A recorded infrared spectrum of the dried residue shows no CN mode, which is consistent with the assumption of the formation of  $\text{NH}_4\text{CN}$ , which sublimates in vacuo at room temperature and would be removed during the removal of liquid  $\text{aNH}_3$ .<sup>[10]</sup> We have therefore put "NH<sub>4</sub>CN" in quotation marks.

Further support for the reaction equation comes from the observations that  $\text{Ag}^+$  is an oxidizing agent<sup>[6,11–14]</sup> and  $\text{U}^{3+}$  is a strong reducing agent, both in liquid ammonia.<sup>[5,15]</sup> An example of its strong reducing capability is the reaction of  $\text{UI}_3$  with

$\text{RbNH}_2$  in  $\text{aNH}_3$ , where  $\text{H}_2$  gas is formed and a blue solution of solvated electrons can be observed.<sup>[16]</sup>

Catena-poly[ $\mu$ -cyanido(tri- $\mu$ -amidodecaammediuranium(IV))] bromide–ammonia(1/2),  $\infty^1[(\mu\text{-CN})\{(\text{H}_3\text{N})_5\text{U}(\mu\text{-NH}_2)_3\text{U}(\text{NH}_3)_5\}]\text{Br}_4 \cdot 2\text{NH}_3$ , crystallizes in the orthorhombic crystal system, space group  $Pmn2_1$  (no. 31) with the lattice parameters  $a = 10.0367(3)$ ,  $b = 12.8161(4)$ ,  $c = 10.8045(4)$  Å,  $V = 1389.80(8)$  Å<sup>3</sup> and  $Z = 2$ , at  $T = 100$  K. Selected crystallographic details are listed in Table 1.

There is one symmetry-independent U atom ( $4b, 1$ ), which is surrounded by three  $\text{NH}_2^-$ , five  $\text{NH}_3$ , and a disordered cyanido ligand in the shape of a tricapped trigonal prism-like polyhedron. The  $\text{NH}_2^-$  ligands bridge between two U atoms to form the  $\{(\text{H}_3\text{N})_5\text{U}(\mu\text{-NH}_2)_3\text{U}(\text{NH}_3)_5\}$  unit in the  $\infty^1[(\mu\text{-CN})\{(\text{H}_3\text{N})_5\text{U}(\mu\text{-NH}_2)_3\text{U}(\text{NH}_3)_5\}]^{4+}$  cation.

The observed U– $\text{NH}_3$  bond lengths lie between 2.586(2) and 2.631(2) Å and agree with those in the  $[\text{U}(\text{NH}_3)_{10}]^{4+}$  cation where 2.5390(15) to 2.621(2) Å were observed.<sup>[6]</sup> The U–( $\mu\text{-NH}_2$ ) distances are with 2.4177(18), 2.4239(19), and 2.440(3) Å, elongated compared to the U– $\text{NH}_2$  bond length of 2.274(15) Å in the compound  $\text{Rb}_2[\text{U}(\text{NH}_2)_6]$  containing only terminally bound  $\text{NH}_2^-$  ligands.<sup>[16]</sup> This elongation is due to  $\mu_2$ -bridging of the  $\text{NH}_2^-$  ligands in the  $\infty^1[(\mu\text{-CN})\{(\text{H}_3\text{N})_5\text{U}(\mu\text{-NH}_2)_3\text{U}(\text{NH}_3)_5\}]^{4+}$  cation. The U...U distance in the  $\{(\text{H}_3\text{N})_5\text{U}(\mu\text{-NH}_2)_3\text{U}(\text{NH}_3)_5\}$  unit is with 3.68490(18) Å quite short but can be explained by the bridging  $\mu\text{-NH}_2^-$  ligands. A possible interaction between these two U atoms is investigated in the quantum-chemical section. The  $\text{CN}^-$  ligand bridges between two  $\{(\text{H}_3\text{N})_5\text{U}(\mu\text{-NH}_2)_3\text{U}(\text{NH}_3)_5\}$  units and is, due to the crystallographic position ( $4d, m..$ ), statistically distorted with a 50:50 mixed site occupancy factor. The U–C/N bond length is 2.597(3) Å, which is, unexpectedly, equal within

the tripled standard uncertainty compared to the  $[\text{U}(\text{CN})(\text{NH}_3)_8]^{3+}$  cation with 2.585(6) Å. Compared to the U–C/N bond length of 2.659(13) Å in the compound  $[\text{U}_2(\text{CN})_3(\text{NH}_3)_{14}][\text{KBr}_6]$ , the one in the  $\infty^1[(\mu\text{-CN})\{(\text{H}_3\text{N})_5\text{U}(\mu\text{-NH}_2)_3\text{U}(\text{NH}_3)_3\}]^{4+}$  cation is shortened, even though both  $\text{CN}^-$  anions are  $\mu_2$ -bridging.<sup>[3]</sup> The observed C–N distance is with 1.165(6) Å in agreement with 1.11(3) Å in the compound  $[\text{U}_2(\text{CN})_3(\text{NH}_3)_{14}][\text{KBr}_6]$ .<sup>[3]</sup> Selected experimentally determined bond lengths are compared to the calculated ones at the DFT-PBE0/TZVP level of theory in Table S7 of the Supporting Information.

Due to the bridging of the  $\text{CN}^-$  unit, an infinite chain is formed, shown in Figure 3. The strings run parallel to the  $a$  axis and can be described with the Niggli formula  $\infty^1[\text{U}(\text{NH}_3)_5(\text{NH}_2)_3(\text{CN})_2]^{2+}$ . The U–CN–U angle is 174.38(11)°, which results in a slightly corrugated chain.

A description of the coordination sphere of the anions, hydrogen bonding, and a packing analysis of the crystal structure is available in the Supporting Information.

Figure 4 shows a Raman spectrum recorded on the green crystals of the compound. It is compared with results of a solid-state DFT calculation at the DFT-PBE0/TZVP level of theory. See computational details for specifics. The calculated wavenum-

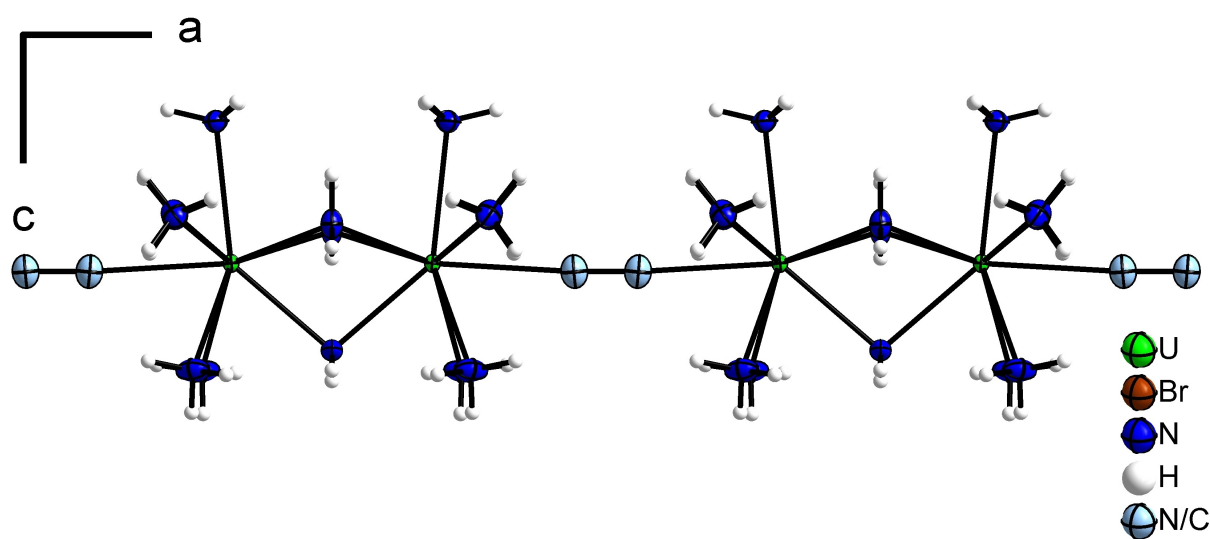


**Figure 3.** Representation of the  $\infty^1[\text{U}(\text{NH}_3)_5(\text{NH}_2)_3(\text{CN})_2]^{2+}$  chain of the bromide running parallel to the  $a$  axis. Anisotropic displacement ellipsoids are shown at the 70% probability level at 100 K. The H atoms are shown isotropic with arbitrary radii.

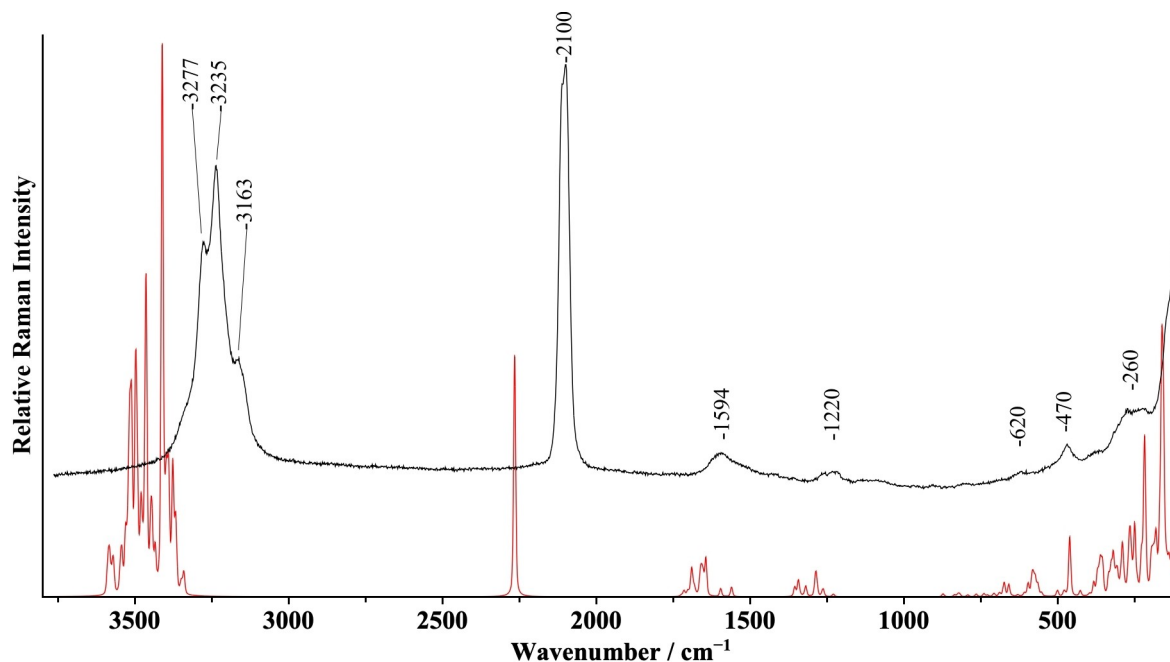


**Figure 4.** Recorded (top, black) and calculated (bottom, red) Raman spectrum of  $\infty^1[(\mu\text{-CN})\{(\text{H}_3\text{N})_5\text{U}(\mu\text{-NH}_2)_3\text{U}(\text{NH}_3)_3\}]\text{Br}_4 \cdot 2\text{NH}_3$ . The recorded spectrum was obtained at room temperature with a 532 nm laser through the glass wall of a bomb tube. Wavenumbers are given for the recorded Raman spectrum.

bers show an overall agreement with the observed ones. Table S6 of the Supporting Information summarizes the band assignments.

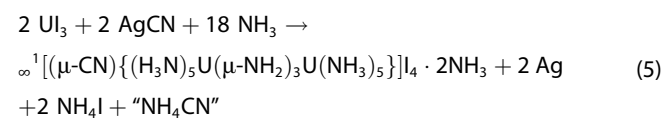
The characteristic  $\nu_s$ -stretching  $C\equiv N$  mode was observed at  $2100\text{ cm}^{-1}$ , which is red-shifted compared to  $2158\text{ cm}^{-1}$  in KCN.<sup>[17]</sup> The observed red-shift is likely due to the coordination of the cyanide unit to the U atoms. This red-shift has been previously observed in several CN-bridged metal complex compounds.<sup>[18]</sup> The calculated wavenumber from DFT is with  $2264\text{ cm}^{-1}$  significantly shifted, but this disagreement can be attributed to the harmonic approximation within the DFT formalism. The modes at  $3277$  and  $3235\text{ cm}^{-1}$  correspond to the  $\nu_{as}$  and  $\nu_s$  stretch modes of the  $\text{NH}_3$  groups, respectively. The band at  $3163\text{ cm}^{-1}$  can be assigned to the  $\nu_s$  N–H mode of the bridging  $\text{NH}_2^-$  ligands. The low-energy modes at  $1594$  and  $1220\text{ cm}^{-1}$  belong to the  $\delta$ -wagging of the  $\text{NH}_3$  groups, while the modes at  $620\text{ cm}^{-1}$  are the  $\delta$ -twisting of the  $\text{NH}_3$  and  $\mu\text{-NH}_2$  groups. Lastly, the mode at  $470\text{ cm}^{-1}$  can be described as the wagging of the  $\text{U}-(\mu\text{-NH}_2)_3\text{-U}$  group. The lower modes describe mostly rotations of  $\text{NH}_3$  molecules and lattice vibrations.

### Synthesis and structural characterization of

#### $\infty^1[(\mu\text{-CN})\{(\text{H}_3\text{N})_5\text{U}(\mu\text{-NH}_2)_3\text{U}(\text{NH}_3)_5\}]_4 \cdot 2\text{NH}_3$

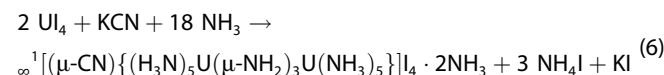
The compound  $\infty^1[(\mu\text{-CN})\{(\text{H}_3\text{N})_5\text{U}(\mu\text{-NH}_2)_3\text{U}(\text{NH}_3)_5\}]_4 \cdot 2\text{NH}_3$  was obtained in two different ways. One was the reaction of  $\text{U}(\text{I})_3$  and  $\text{AgCN}$  in 1:1 ratio at  $40^\circ\text{C}$  in liquid  $\text{aNH}_3$  in a bomb tube, where after six days, green blocks of suitable size for an X-ray diffraction experiment were observed. The results of the structure determination on crystals from this route will be presented in the following. In the second synthetic approach,  $\text{U}(\text{I})_4$  was reacted with KCN in a 1:1 ratio in liquid  $\text{aNH}_3$  at room temperature in a bomb tube. Green crystals of suitable size for an X-ray diffraction experiment were obtained after two weeks of crystallization time. Unfortunately, the crystal and the recorded data set were of very low quality and only the determined lattice parameters are given in the Supporting Information.

For the first approach, reaction equation 5 can be formulated.



According to equation 4,  $\text{U}^{3+}$  is oxidized while  $\text{Ag}^+$  is reduced. The side product  $\text{NH}_4\text{I}$  was identified by powder X-ray diffraction on the dried left-overs of  $\infty^1[(\mu\text{-CN})\{(\text{H}_3\text{N})_5\text{U}(\mu\text{-NH}_2)_3\text{U}(\text{NH}_3)_5\}]_4 \cdot 2\text{NH}_3$  after the evaporation of the liquid  $\text{aNH}_3$ . The diffraction pattern is shown in Figure S7 of the Supporting Information. Ag metal was observed as it formed as a mirror on the inner wall of the reaction vessel during the reaction. A photograph is shown in the Supporting Information in Figure S9. For the balance of the reaction equation, the formation of  $\text{NH}_4\text{CN}$  is assumed, as discussed above.

The second synthesis can be described by reaction equation 6.



The formation of  $\text{NH}_4\text{I}$  and  $\text{KI}$  have been traced by powder X-ray diffraction on the dried left-overs of  $\infty^1[(\mu\text{-CN})\{(\text{H}_3\text{N})_5\text{U}(\mu\text{-NH}_2)_3\text{U}(\text{NH}_3)_5\}]_4 \cdot 2\text{NH}_3$  after the evaporation of liquid  $\text{aNH}_3$ . The diffraction pattern is shown in Figure S8 in the Supporting Information.

Catena-poly[ $\mu$ -cyanido(tri- $\mu$ -amidodecaammediuranium(IV))] iodide–ammonia(1/2),  $\infty^1[(\mu\text{-CN})\{(\text{H}_3\text{N})_5\text{U}(\mu\text{-NH}_2)_3\text{U}(\text{NH}_3)_5\}]_4 \cdot 2\text{NH}_3$ , crystallizes in the orthorhombic crystal system, in space group *Imm2* (no. 44) with the lattice parameters  $a = 13.6703(9)$ ,  $b = 10.1319(6)$ ,  $c = 10.8507(7)\text{ \AA}$ ,  $V = 1502.89(16)\text{ \AA}^3$  and  $Z = 2$ , at  $T = 100\text{ K}$ . In Table 1 selected crystallographic details are listed.

We note that the compounds  $\infty^1[(\mu\text{-CN})\{(\text{H}_3\text{N})_5\text{U}(\mu\text{-NH}_2)_3\text{U}(\text{NH}_3)_5\}]\text{Br}_4 \cdot 2\text{NH}_3$  and  $\infty^1[(\mu\text{-CN})\{(\text{H}_3\text{N})_5\text{U}(\mu\text{-NH}_2)_3\text{U}(\text{NH}_3)_5\}]_4 \cdot 2\text{NH}_3$  both crystallize in the orthorhombic crystal system, but with different centering, *oP* versus *ol*, respectively. Both structures are strongly related and may be isotypic. However, our X-ray diffraction data are not good enough to unambiguously resolve this issue. A detailed discussion on the crystallographic details, choice of centering and space groups, is given in the Supporting Information.

The crystal structure of  $\infty^1[(\mu\text{-CN})\{(\text{H}_3\text{N})_5\text{U}(\mu\text{-NH}_2)_3\text{U}(\text{NH}_3)_5\}]_4 \cdot 2\text{NH}_3$  contains one symmetry independent U atom (*4d*, *m.*) which is surrounded by three  $\text{NH}_2^-$ , five  $\text{NH}_3$ , and a  $\text{CN}^-$  ligand, to form a tricapped trigonal prism-like coordination sphere. It closely resembles the one observed in the  $\infty^1[(\mu\text{-CN})\{(\text{H}_3\text{N})_5\text{U}(\mu\text{-NH}_2)_3\text{U}(\text{NH}_3)_5\}]\text{Br}_4 \cdot 2\text{NH}_3$  compound above. The five U– $\text{NH}_3$  distances range from  $2.590(3)$  to  $2.632(3)\text{ \AA}$ , which agree with the observed distances for the  $[\text{U}(\text{NH}_3)_{10}]^{4+}$  cation.<sup>[6]</sup> The three U– $\text{NH}_2$  bond lengths are  $2 \times 2.407(3)$  and  $2.445(6)\text{ \AA}$ , which agree with distances observed in the compounds  $\infty^1[(\mu\text{-CN})\{(\text{H}_3\text{N})_5\text{U}(\mu\text{-NH}_2)_3\text{U}(\text{NH}_3)_5\}]\text{Br}_4 \cdot 2\text{NH}_3$  and  $\text{Rb}_2[\text{U}(\text{NH}_2)_6]$ .<sup>[16]</sup> The U–C/N bond length is with  $2.628(4)\text{ \AA}$  significantly elongated compared to  $2.597(3)\text{ \AA}$  in the Br compound, however agrees with the U–C/N distances of  $2.659(13)\text{ \AA}$  in the compound  $[\text{U}_2(\text{CN})_3(\text{NH}_3)_{14}][\text{KBr}_6]$ .<sup>[3]</sup> Furthermore, the C–N distance is with  $1.178(8)\text{ \AA}$  comparable to  $1.165(6)\text{ \AA}$  in the related bromide. Similar to the bromide, the  $\infty^1[\text{U}(\text{NH}_3)_5(\text{NH}_2)_2(\text{CN})_2]^{2+}$  cations of the iodide form infinite strands.

A description of the coordination sphere of the anions, hydrogen bonding, and a packing analysis of the crystal structure is available in the Supporting Information.

### Quantum-chemical considerations for the $[\{(\text{NH}_3)_5\text{U}(\mu\text{-NH}_2)_3\text{U}(\text{CN})\}]^{4+}$ cation

As a first example of a heteroleptic U complex cation containing a  $\text{CN}^-$  ligand and  $\text{NH}_2^-$  ligands, we were interested in the energetic differences between the linkage-isomers U–CN and U–NC as well as in the bonding situation of the U–( $\mu\text{-NH}_2$ ) and

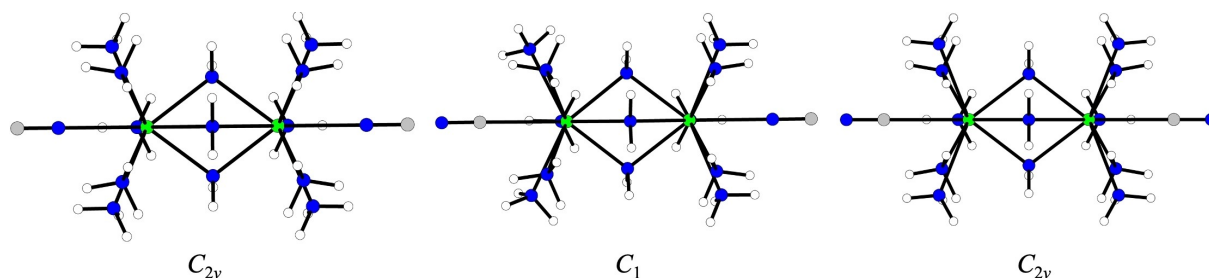


**Figure 5.** Different linkage-isomers,  $\kappa\text{C}$  and  $\kappa\text{N}$ , of the complex cation  $[(\mu\text{-CN})_2\{(\text{H}_3\text{N})_5\text{U}(\mu\text{-NH}_2)_3\text{U}(\text{NH}_3)_5\}]^{3+}$ . Idealized point groups given underneath each structure. Left:  $\kappa\text{N}$ -,  $\kappa\text{N}$ -isomer. Middle:  $\kappa\text{N}$ -,  $\kappa\text{C}$ -isomer. Right:  $\kappa\text{C}$ -,  $\kappa\text{C}$ -isomer. C atoms in grey, N atoms in blue, H atoms in white, U atoms in green color.

U–C/N units. We therefore calculated the molecular  $[(\mu\text{-CN})_2\{(\text{H}_3\text{N})_5\text{U}(\mu\text{-NH}_2)_3\text{U}(\text{NH}_3)_5\}]^{3+}$  cation (two CN<sup>−</sup> units per  $\{(\text{H}_3\text{N})_5\text{U}(\mu\text{-NH}_2)_3\text{U}(\text{NH}_3)_5\}$  unit) as a model system at the DFT-PBE0/TZVP level of theory. Solvent effects were not explicitly considered in the calculations, but implicit COSMO solvent model, was used to counter the charges.

Figure 5 shows the different linkage-isomers,  $\kappa\text{C}$  and  $\kappa\text{N}$  for the model cation  $[(\mu\text{-CN})_2\{(\text{H}_3\text{N})_5\text{U}(\mu\text{-NH}_2)_3\text{U}(\text{NH}_3)_5\}]^{3+}$ .

The  $\kappa\text{N}$ -,  $\kappa\text{N}$ -isomer shown on the left of Figure 5, and the  $\kappa\text{N}$ -,  $\kappa\text{C}$ -linkage-isomer in the middle are isoenergetic at 0 K. In contrast, the  $\kappa\text{C}$ -,  $\kappa\text{C}$ -isomer, shown on the right in Figure 5, is 33 kJ·mol<sup>−1</sup> higher in energy compared to the other two structures. These findings are in line with those for the  $[\text{U}(\text{CN})(\text{NH}_3)_8]^{3+}$  cation, where the  $\kappa\text{N}$ - is favored over the  $\kappa\text{C}$ -linkage-isomer by 23 kJ·mol<sup>−1</sup> at 0 K.

Due to the quite short U...U distance of 3.68490(18) Å in the  $\{(\text{H}_3\text{N})_5\text{U}(\mu\text{-NH}_2)_3\text{U}(\text{NH}_3)_5\}$  unit, we calculated the energy difference between the quintet state,  $S=2$ , and the singlet state,  $S=0$ , which appeared to be 0 kJ·mol<sup>−1</sup>. This excludes an interaction between the U atoms.

The  $\kappa\text{N}$ -,  $\kappa\text{C}$ -linkage-isomer will be used to discuss the IBOs of the  $[\{(\text{NH}_3)_5\text{U}\}_2(\mu\text{-NH}_2)_3(\text{CN})_2]^{3+}$  cation. There are six IBOs describing the  $\sigma$ -type bonds between U–( $\mu\text{-NH}_2$ ), which also contain a  $\pi$ -interaction towards the second U atom. One of these IBOs is shown in Figure 6.

The N atom contributes with 80% to the U–( $\mu\text{-NH}_2$ ) IBO, while the U atoms participate either with 16% to the  $\sigma$ -type IBO

or with 3% in a  $\pi$ -type interaction. The IBOs describing the U–N/C interaction are with contributions of the C/N atom of 86% for U–N and 82% for U–C, respectively, slightly more ionic compared to the U–( $\mu\text{-NH}_2$ ) bond. These findings coincide with the one for the  $[\text{U}(\text{CN})(\text{NH}_3)_8]^{3+}$  cation. In conclusion, the U–( $\mu\text{-NH}_2$ ) and U–C/N interactions seem to be quite ionic  $\sigma$ -type bonds, while in case of the U–( $\mu\text{-NH}_2$ ) bond a  $\pi$ -type interaction towards the second U atom is present. A detailed discussion on the orbital contributions is handed in the IBO section of the Supporting Information.

## Conclusions

The reaction of KCN with  $\text{UCl}_4$  resulted in the formation of the compound  $[\text{U}(\text{CN})(\text{NH}_3)_8]\text{Cl}_3 \cdot 3\text{NH}_3$ , which is the first example for a monocyanido uranium(IV) complex formed from liquid  $\text{aNH}_3$  solution. A quantum-chemical investigation on the bonding situation of the  $[\text{U}(\text{CN})(\text{NH}_3)_8]^{3+}$  cation revealed a  $\sigma$ -type U–CN bond with a quite ionic character. The orbital contributions of the U atom are comparable to related complex cations like  $[\text{UCl}(\text{NH}_3)_8]^{3+}$ .

The oxidation of the uranium(III) halides,  $\text{UBr}_3$  and  $\text{UI}_3$ , in the presence of AgCN led to the formation of unprecedented polymeric chain cations  $[\{(\mu\text{-CN})\{(\text{H}_3\text{N})_5\text{U}(\mu\text{-NH}_2)_3\text{U}(\text{NH}_3)_5\}]^{4+}$  in the compounds  $[\{(\mu\text{-CN})\{(\text{H}_3\text{N})_5\text{U}(\mu\text{-NH}_2)_3\text{U}(\text{NH}_3)_5\}]\text{Br}_4 \cdot 2\text{NH}_3$  and  $[\{(\mu\text{-CN})\{(\text{H}_3\text{N})_5\text{U}(\mu\text{-NH}_2)_3\text{U}(\text{NH}_3)_5\}]\text{I}_4 \cdot 2\text{NH}_3$ . Quantum-chemical

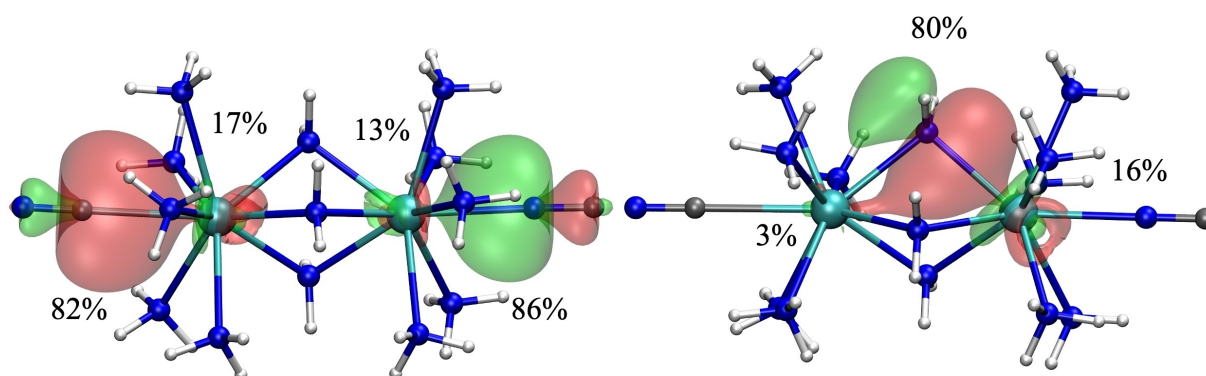


**Figure 6.** Two sets of IBOs for the  $\kappa\text{N}$ -,  $\kappa\text{C}$ - $[\{(\text{NH}_3)_5\text{U}\}_2(\mu\text{-NH}_2)_3(\text{CN})_2]^{3+}$  cation (isosurfaces drawn in green and red). Left:  $\sigma$ -type IBO between U–C/N. Right: One of the  $\sigma$ -type IBOs between U–( $\mu\text{-NH}_2$ ), with the  $\pi$ -interaction towards the second U atom. The listed percentages show the contribution of each atom in the IBO. In a purely covalent 2c-bond, each atom would contribute 50%. Atomic contributions smaller than 2% to any IBO are not listed. The isovalue for IBO isosurface plots is 0.03 a.u. U atoms in cyan, N atoms in blue, C atoms in grey, and H atoms in white color.

investigations on the bonding situation of the  $\mu\text{-NH}_2^-$  and  $\mu\text{-CN}^-$  ligands towards the U atoms showed quite ionic interactions. In addition to the  $\sigma$ -type U–( $\mu\text{-NH}_2$ ) bonds additional  $\pi$ -type interactions towards the second U atom are present.

## Experimental Details

All work was carried under argon atmosphere (5.0, Praxair) using a fine-vacuum line and a glovebox (MBraun). Liquid ammonia was dried by storage over Na. The self-made borosilicate glass bomb tubes for the reactions with liquid ammonia were flame-dried at least three times before use. The uranium containing starting materials  $\text{UBr}_3$ ,  $\text{U}_3$ ,  $\text{UCl}_4$ , and  $\text{U}_4$  were prepared as described previously.<sup>[19,20]</sup> All compounds obtained here are unstable at room temperature due to loss of  $\text{NH}_3$ . Therefore, no further analyses, such as elemental analyses, could be carried out. For the same reason, yields could not be determined.

### Preparation of $[\text{U}(\text{CN})(\text{NH}_3)_8]\text{Cl}_3 \cdot 3\text{NH}_3$

A borosilicate bomb tube was charged with 58.3 mg  $\text{UCl}_4$  (0.154 mmol) and 10 mg KCN (0.154 mmol), filled with approximately 2 mL liquid  $\text{NH}_3$ , cooled to liquid nitrogen temperature, flame-sealed, and stored at room temperature. A few green crystals were obtained which had grown large enough for X-ray diffraction experiments after one month. After removal of the residual liquid  $\text{NH}_3$  in vacuo at room temperature, a greenish powder remained. Its diffraction pattern is shown in the Supporting Information in Figure S5.

### Preparation of $\infty^1[(\mu\text{-CN})\{(\text{H}_3\text{N})_5\text{U}(\mu\text{-NH}_2)_3\text{U}(\text{NH}_3)_5\}]\text{Br}_4 \cdot 2\text{NH}_3$

A borosilicate bomb tube was charged with 20 mg  $\text{UBr}_3$  (0.04 mmol) and 6 mg  $\text{AgCN}$  (0.04 mmol), filled with approximately 2 mL liquid  $\text{NH}_3$ , cooled to liquid nitrogen temperature, flame-sealed, and stored at 40 °C. After 10 months, a few green crystals of suitable size for single-crystal X-ray diffraction were obtained. After removal of residual liquid  $\text{NH}_3$  in vacuo at room temperature, a greyish powder remained. The diffraction pattern is shown in the Supporting Information in Figure S6.

### Preparation of $\infty^1[(\mu\text{-CN})\{(\text{H}_3\text{N})_5\text{U}(\mu\text{-NH}_2)_3\text{U}(\text{NH}_3)_5\}]\text{I}_4 \cdot 2\text{NH}_3$

The compound has been obtained in two different ways:

- 1) A borosilicate bomb tube was charged with 20 mg  $\text{U}_3$  (0.03 mmol) and 4 mg  $\text{AgCN}$  (0.03 mmol), filled with approximately 2 mL liquid  $\text{NH}_3$ , cooled to liquid nitrogen temperature, flame-sealed, and stored at 40 °C. After six days, green crystals had grown large enough for X-ray diffraction experiments. Overall, only a few crystals of the compound were obtained. After removal of the residual liquid  $\text{NH}_3$  in vacuo at room temperature, a greyish powder remained. The diffraction pattern is shown in the Supporting Information in Figure S7.
- 2) A borosilicate bomb tube was charged with 114.5 mg  $\text{U}_4$  (0.154 mmol) and 10 mg KCN (0.154 mmol), filled with approximately 2 mL liquid  $\text{NH}_3$ , cooled to liquid nitrogen temperature, flame-sealed, and stored at room temperature. After two weeks, green crystals had grown large enough for X-ray diffraction experiments. Unfortunately, only one crystal of low quality was used. The unit cell determination was conducted on an IPDS2T diffractometer (Stoe & Cie). Only a few crystals of the compound have been yielded. After removal of the residual liquid  $\text{NH}_3$  in

vacuo at room temperature, a greenish powder remained. Its diffraction pattern is shown in the Supporting Information in Figure S8.

### Raman spectroscopy

The Raman spectrum was recorded through the glass wall of the bomb tube at room temperature with a Monovista CRS+ confocal Raman microscope (Spectroscopy & Imaging GmbH) using a solid-state laser with  $\lambda = 532$  nm and a 300 grooves/mm (low-resolution mode, FWHM:  $< 4.62$   $\text{cm}^{-1}$ ) grating.

### IR spectroscopy

The IR spectra of the dried residues were recorded on a Bruker alpha FT-IR spectrometer using the ATR Diamond module with a resolution of  $4$   $\text{cm}^{-1}$ . The spectrometer was located inside a glovebox (MBraun) under argon atmosphere. The spectra were processed with the OPUS software package.<sup>[21]</sup>

### Powder X-ray diffraction

The samples of the dried residues were filled into a flame-dried borosilicate glass capillaries with a diameter of 0.3 mm. The powder X-ray diffraction patterns were recorded with a StadiMP diffractometer (Stoe & Cie) in Debye-Scherrer geometry. The diffractometer was operated with  $\text{Cu-K}\alpha_1$  radiation (1.5406 Å, germanium monochromator) and equipped with a MYTHEN 1K detector. The diffraction patterns were processed using the WinXPOW suite.<sup>[22]</sup>

### Single-crystal X-ray diffraction

$\infty^1[(\mu\text{-CN})\{(\text{H}_3\text{N})_5\text{U}(\mu\text{-NH}_2)_3\text{U}(\text{NH}_3)_5\}]\text{Br}_4 \cdot 2\text{NH}_3$  and  $\infty^1[(\mu\text{-CN})\{(\text{H}_3\text{N})_5\text{U}(\mu\text{-NH}_2)_3\text{U}(\text{NH}_3)_5\}]\text{I}_4 \cdot 2\text{NH}_3$  crystals were selected under nitrogen-cooled, pre-dried perfluorinated oil (Galden HT270, PFPE, Solvey Solexis) and under the absence of air. The crystals were mounted with a MiTeGen loop. Intensity data of suitable crystals were recorded with a D8 Quest diffractometer (Bruker). The diffractometer was operated with monochromatized  $\text{Mo-K}\alpha$  radiation (0.71073 Å, multi layered optics) and equipped with a PHOTON III C14 detector. Evaluation, integration, and reduction of the diffraction data was carried out with the APEX4 software suite.<sup>[23]</sup> The diffraction data were corrected for absorption utilizing the multi-scan method of SADABS within the APEX4 software suite. The structures were solved with dualspace methods (SHELXT) and refined against  $F^2$  (SHELXL).<sup>[24,25]</sup> All atoms were refined with anisotropic displacement parameters, H atoms were either located from the Difference Fourier map and refined isotropic, or with a riding model, or fixed, in some structures some H atoms could not be positioned. Representations of the crystal structures were created with the Diamond software.<sup>[26]</sup>

$[\text{U}(\text{CN})(\text{NH}_3)_8]\text{Cl}_3 \cdot 3\text{NH}_3$  crystals were selected under nitrogen-cooled, pre-dried perfluorinated oil (Galden HT270, PFPE, Solvey Solexis) and under the absence of air. The crystals were mounted with a MiTeGen loop. Intensity data of suitable crystals were recorded with an IPDS 2T diffractometer (Stoe & Cie). The diffractometer was operated with  $\text{Mo-K}\alpha$  radiation (0.71073 Å, graphite monochromator) and equipped with an image plate detector. Evaluation, integration, and reduction of the diffraction data were carried out using the X-Area software suite.<sup>[27]</sup> Numerical absorption corrections were applied with the modules X-Shape and X-Red32 of the X-Area software suite. The structures were solved with dual space methods (SHELXT) and refined against  $F^2$  (SHELXL). All atoms were refined

with anisotropic displacement parameters, H atoms were either located from the Difference Fourier map and refined isotropic, or with a riding model, or fixed. In some structures some H atoms could not be positioned. Representations of the crystal structure were created with the Diamond software.

Deposition Numbers 2311396 for  $[\text{U}(\text{CN})(\text{NH}_3)_8]\text{Cl}_3 \cdot 3\text{NH}_3$ , 2311398 for  $[\mu\text{-CN}]\{(\text{H}_3\text{N})_5\text{U}(\mu\text{-NH}_2)_3\text{U}(\text{NH}_3)_5\}\text{Br}_4 \cdot 2\text{NH}_3$ , 2311397 for  $[\mu\text{-CN}]\{(\text{H}_3\text{N})_5\text{U}(\mu\text{-NH}_2)_3\text{U}(\text{NH}_3)_5\}\text{I}_4 \cdot 2\text{NH}_3$  contain(s) the supplementary crystallographic data for this paper. These data are provided free of charge by the joint Cambridge Crystallographic Data Centre and Fachinformationszentrum Karlsruhe Access Structures service.

## Computational Details

Molecular Density Functional Theory (DFT) calculations were carried out with the TURBOMOLE7.7<sup>[28,29]</sup> program suite using the PBE0 hybrid density functional method (DFT-PBE0).<sup>[30,31]</sup> We used def-TZVP triple- $\zeta$ -valence basis sets for hydrogen, carbon, and oxygen atoms.<sup>[32]</sup> For the uranium atom, scalar relativistic effects were taken into account using a 60-electron effective core potential (ECP) combined with def-TZVP triple- $\zeta$ -valence basis set.<sup>[33–35]</sup> Multipole-accelerated resolution-of-the-identity approximation (MA-RIJ) was used to speed up the DFT calculations<sup>[36–38]</sup> and a m4 integration grid was used for the numerical integration of the exchange-correlation part. The “COnductor-like Screening MOdel” (COSMO) was applied to all structures to compensate for their positive charges (dielectric constant of infinity was used).<sup>[39]</sup> The structures of the complex cations were fully optimized within the constraints of their respective molecular point group symmetry. Numerical harmonic frequency calculations were performed to check if the optimized structures were true local minima on the potential energy surfaces. The Cartesian coordinates of the optimized structures are available from the Supporting Information. Intrinsic bond orbital (IBO) analyses were performed with the Turbomole module *proper*.<sup>[8]</sup> A previously published  $\text{U}^{40}$  reference basis set was used for the IBO analysis. Gibbs Free Energies were obtained within the harmonic oscillator rigid rotor model at room temperature, using the *freeh* module. The harmonic frequencies were not scaled when evaluating the thermal contributions.

Periodic quantum-chemical calculations were conducted using the CRYSTAL23 software suite.<sup>[41]</sup> The DFT-PBE0 hybrid density functional method (PBE+25% exact HF exchange) was used in all calculations.<sup>[30,31]</sup> Gaussian-type triple- $\zeta$ -valence + polarization basis sets (TZVP) were applied for all elements. The basis sets have been derived from the Karlsruhe basis sets and the U basis includes a 60-electron scalar relativistic effective core potential.<sup>[34,42]</sup> The basis sets for U, H, N, C, and Br have been published previously.<sup>[16,43,44]</sup> More specifics are reported in the Supporting Information.

## Supporting Information

The Supporting Information contains further crystallographic details, the powder X-ray diffraction patterns, the IR spectra, details of the quantum-chemical calculations.<sup>[45–49]</sup>

## Acknowledgements

T. G. thanks the HPC-EUROPA3 (INFRAIA-2016-1-730897) for a travel grant and the computing resources provided by CSC, the Finnish IT Center for Science. T. G. thanks D. Witzel for

conducting some experiments. We thank the IAEA and the Euratom for reading our manuscript that contains the terms uranium and bomb several times. F. K. thanks the Deutsche Forschungsgemeinschaft, KR3595/13-1, for funding. Open Access funding enabled and organized by Projekt DEAL.

## Conflict of Interests

The authors declare no conflict of interest.

## Data Availability Statement

The data that support the findings of this study are available in the supplementary material of this article.

**Keywords:** Uranium · cyanide · quantum-chemical calculation · liquid ammonia

- [1] H. Hennig, A. Rehorek, D. Rehorek, Ph. Thomas, *Inorg. Chim. Acta* **1984**, *86*, 41–49.
- [2] K. W. Bagnall, J. L. Baptista, *J. Inorg. Nucl. Chem.* **1970**, *32*, 2283–2285.
- [3] H. L. Deubner, F. Kraus, *Z. Naturforsch.* **2020**, *75*, 111–116.
- [4] S. S. Rudel, C. Pietzonka, M. Hoelzel, F. Kraus, *Chem. Commun.* **2018**, *54*, 1241–1244.
- [5] S. S. Rudel, S. A. Baer, P. Woidy, T. G. Müller, H. L. Deubner, B. Scheibe, F. Kraus, *Z. Kristallogr.* **2018**, *233*, 817–844.
- [6] S. S. Rudel, H. L. Deubner, T. G. Müller, T. Graubner, S. I. Ivlev, F. Kraus, *Z. Anorg. Allg. Chem.* **2022**, *648*, e202200211.
- [7] N. Elliott, J. Hastings, *Acta Crystallogr.* **1961**, *14*, 1018–1018.
- [8] G. Knizia, *J. Chem. Theory Comput.* **2013**, *9*, 4834–4843.
- [9] H. L. Deubner, T. Graubner, F. Weigend, A. J. Karttunen, F. Kraus, *Eur. J. Inorg. Chem.* **2021**, *27*, 2787–2796.
- [10] E. S. Dodsworth, J. P. Eaton, M. P. Ellerby, D. Nicholls, *Inorg. Chim. Acta* **1984**, *89*, 143–145.
- [11] R. J. Kline, C. J. Kershner, *Inorg. Chem.* **1966**, *5*, 932–934.
- [12] T. G. Müller, F. Karau, W. Schnick, F. Kraus, *Angew. Chem. Int. Ed.* **2014**, *53*, 13695–13697.
- [13] T. G. Müller, M. R. Buchner, T. J. Scheubeck, N. Korber, F. Kraus, *Z. Anorg. Allg. Chem.* **2016**, *642*, 796–803.
- [14] T. G. Müller, J. Mogk, M. Conrad, F. Kraus, *Eur. J. Inorg. Chem.* **2016**, *2016*, 4162–4169.
- [15] W. Burk, *Z. Anorg. Allg. Chem.* **1967**, *350*, 62–69.
- [16] S. S. Rudel, A. J. Karttunen, F. Kraus, *Z. Anorg. Allg. Chem.* **2020**, *646*, 1023–1029.
- [17] G. E. Leroi, W. Klemperer, *J. Chem. Phys.* **1961**, *35*, 774–775.
- [18] S. F. A. Kettle, E. Diana, E. M. C. Marchese, E. Boccaleri, G. Croce, T. Sheng, P. L. Stanghellini, *Eur. J. Inorg. Chem.* **2010**, *2010*, 3920–3929.
- [19] S. S. Rudel, F. Kraus, *Dalton Trans.* **2017**, *46*, 5835–5842.
- [20] S. S. Rudel, H. L. Deubner, B. Scheibe, M. Conrad, F. Kraus, *Z. Anorg. Allg. Chem.* **2018**, *644*, 323–329.
- [21] OPUS V7.2, Bruker Optik GmbH, Ettlingen, Germany, **2012**.
- [22] WinXPOW V3.11, STOE, Darmstadt, Germany, **2018**.
- [23] APEX4 V2022.10-0, Bruker AXS Inc., Madison, Wisconsin, USA, **2022**.
- [24] G. M. Sheldrick, *Acta Crystallogr.* **2015**, *A71*, 3–8.
- [25] G. M. Sheldrick, *Acta Crystallogr.* **2015**, *C71*, 3–8.
- [26] K. Brandenburg, H. Putz, *Diamond - Crystal and Molecular Structure Visualization*, V 4.6.8, Crystal Impact GbR, Bonn, **2022**.
- [27] X-Area 1.8.1, STOE & Cie GmbH, Darmstadt, Germany, **2018**.
- [28] R. Ahlrichs, M. Bär, M. Häser, H. Horn, C. Kölmel, *Chem. Phys. Lett.* **1989**, *162*, 165–169.
- [29] TURBOMOLE V7.7, a Development of University of Karlsruhe and Forschungszentrum Karlsruhe GmbH, 1989–2007, TURBOMOLE GmbH, since 2007, **2022**.
- [30] C. Adamo, V. Barone, *J. Chem. Phys.* **1999**, *110*, 6158–6170.
- [31] J. P. Perdew, K. Burke, M. Ernzerhof, *Phys. Rev. Lett.* **1996**, *77*, 3865–3868.
- [32] F. Weigend, R. Ahlrichs, *Phys. Chem. Phys.* **2005**, *7*, 3297–3305.

- [33] A. Schäfer, C. Huber, R. Ahlrichs, *J. Chem. Phys.* **1994**, *100*, 5829–5835.
- [34] W. Küchle, M. Dolg, H. Stoll, H. Preuss, *J. Chem. Phys.* **1994**, *100*, 7535–7542.
- [35] X. Cao, M. Dolg, H. Stoll, *J. Chem. Phys.* **2003**, *118*, 487–496.
- [36] F. Weigend, *Phys. Chem. Chem. Phys.* **2002**, *4*, 4285–4291.
- [37] K. Eichkorn, O. Treutler, H. Öhm, M. Häser, R. Ahlrichs, *Chem. Phys. Lett.* **1995**, *240*, 283–290.
- [38] M. Sierka, A. Hogekamp, R. Ahlrichs, *J. Chem. Phys.* **2003**, *118*, 9136–9148.
- [39] A. Klamt, G. Schürmann, *J. Chem. Soc. Perkin Trans. 2* **1993**, 799–805.
- [40] S. S. Rudel, H. L. Deubner, M. Müller, A. J. Karttunen, F. Kraus, *Nat. Chem.* **2020**, *12*, 962–967.
- [41] A. Erba, J. K. Desmarais, S. Casassa, B. Civalleri, L. Donà, I. J. Bush, B. Searle, L. Maschio, L. Edith-Daga, A. Cossard, C. Ribaldone, E. Ascrizzi, N. L. Marana, J.-P. Flament, B. Kirtman, *J. Chem. Theory Comput.* **2023**, *19*, 6891–6932.
- [42] X. Cao, M. Dolg, *J. Mol. Struct.: THEOCHEM* **2004**, *673*, 203–209.
- [43] A. J. Karttunen, T. Tynell, M. Karppinen, *J. Phys. Chem. C* **2015**, *119*, 13105–13114.
- [44] S. I. Ivlev, K. Gaul, M. Chen, A. J. Karttunen, R. Berger, F. Kraus, *Chem. Eur. J.* **2019**, *25*, 5793–5802.
- [45] H. J. Monkhorst, J. D. Pack, *Phys. Rev. B* **1976**, *13*, 5188–5192.
- [46] R. Dovesi, A. Erba, R. Orlando, C. M. Zicovich-Wilson, B. Civalleri, L. Maschio, M. Rérat, S. Casassa, J. Baima, S. Salustro, B. Kirtman, *Wiley Interdiscip. Rev.: Comput. Mol. Sci.* **2018**, *8*, e1360.
- [47] F. Pascale, C. M. Zicovich-Wilson, F. López Gejo, B. Civalleri, R. Orlando, R. Dovesi, *J. Comput. Chem.* **2004**, *25*, 888–897.
- [48] L. Maschio, B. Kirtman, M. Rérat, R. Orlando, R. Dovesi, *J. Chem. Phys.* **2013**, *139*, 164102.
- [49] H. T. Stokes, D. M. Hatch, *J. Appl. Crystallogr.* **2005**, *38*, 237–238.

Manuscript received: January 22, 2024

Revised manuscript received: February 8, 2024

Accepted manuscript online: February 8, 2024

Version of record online: February 23, 2024